Available online at www.sciencedirect.com
SCIENCE DIRECT
ELSEVIER
Ultramicroscopy 106 (2006) 475–479
ultramicroscopy
www.elsevier.com/locate/ultramic

Wide angle near-field optical probes by reverse tube etching

S. Patanè[a,*], E. Cefalì[a], A. Arena[a], P.G. Gucciardi[b], M. Allegrini[c]

[a]*Dipartimento di Fisica della Materia e Tecnologie Fisiche Avanzate, Università di Messina, Salita Sperone 31, 98166 Messina, Italy*
[b]*CNR-Istituto per i Processi Chimico Fisici sez. di Messina, Via la Farina 237, 98123 Messina, Italy*
[c]*Dipartimento di Fisica "Enrico Fermi", Università di Pisa, Largo Bruno Pontecorvo 3, 56127 Pisa, Italy*

Received 4 July 2005; received in revised form 19 December 2005; accepted 12 January 2006

Abstract

We present a simple modification of the tube etching process for the fabrication of fiber probes for near-field optical microscopy. It increases the taper angle of the probe by a factor of two. The novelty is that the fiber is immersed in hydrofluoric acid and chemically etched in *an upside-down geometry*. The tip formation occurs inside the micrometer tube cavity formed by the polymeric jacket. By applying this approach, called reverse tube etching, to multimode fibers with 200/250 μm core/cladding diameter, we have fabricated tapered regions featuring high surface smoothness and average cone angles of ~30°. A simple model based on the crucial role of the gravity in removing the etching products, explains the tip formation process.
© 2006 Elsevier B.V. All rights reserved.

Keywords: Optical probes; Tube etching

1. Introduction

Near-field scanning optical microscopy (SNOM) is a well-assessed technique that combines scanning probe technologies with optical microscopy to overcome the diffraction limit. It is an important characterization tool in materials science and in biology. It is also suitable for applications as nano-optical lithography and great efforts have been devoted to the improvement of its performances [1]. The aperture SNOM, where the near field is produced by light passing through a hole whose dimension is smaller than the light wavelength, is the most common version of the microscope. The probes are usually optical fibers, tapered and metal coated at one end. Unfortunately, when the fiber diameter becomes smaller than half of the light wavelength, the optical mode is no longer able to propagate and it goes in the cutoff regime where the intensity decreases exponentially. Thus, these probes transmit very little light through the aperture, but they provide perfect suppression of background radiation. The characteristics of the probe are of the utmost importance to the performances of the instrument. A larger aperture increases the optical throughput but this improvement is only apparent because the resolution is reduced with the loss of the high spatial frequency components of the electromagnetic field produced by the probe.

In this frame, the cone angle of the apex plays a fundamental role in order to reduce the propagation path for the evanescent field inside the fiber as well as the losses due to the multiple internal reflection. A larger cone produces a more efficient probe while preserving the resolution.

Probes suitable for near-field optical microscopy are commercially available from several companies. Their production, usually requires two steps. The first one consists in producing the conical apex and it is usually accomplished by the so-called "heating and pulling" method [2], or by alternative processes such as the chemical etching [3], or by bevelling the optical fiber [4]. In the second step the fiber is metallized to obtain the optical confinement and the nanometric aperture at the apex of the tip [1]. The heating and pulling method produces tips with

*Corresponding author. Tel.: +390903977373; fax: +39090391382.
E-mail addresses: patanes@unime.it, salvatore.patane@unime.it (S. Patanè).

0304-3991/$ - see front matter © 2006 Elsevier B.V. All rights reserved.
doi:10.1016/j.ultramic.2006.01.002

small cone angle and a quite smooth surface. A regular surface is one of the qualifying characteristic of the heating and pulling method that provides a metallization without pin holes. However, in this case the throughput is low, ranging from 10^{-8} to 10^{-5} and it depends on the final aperture of the probe [2]. The chemical etching, also known as "*Turner method*" [3] is simpler and low cost. It produces wider cone angles and the tip length is reduced to a few hundreds microns. This procedure consists in dipping the fiber core, without any jacket, in an hydrofluoridric solution covered by an organic solvent. The tip is obtained because of the meniscus formed on the fiber walls and the acid–solvent interface. During the etching, the fiber is consumed as long as it remains inside the acid. This method is able to produce angles wider than those obtained by pulling together with a larger throughput of about 10^{-3} [4–6]. The simplicity of the method is paid in terms of surface roughness, that leads to the formation of some pin holes populating the metallic coating and results in lower quality and reproducibility of the probes [7]. Several authors have proposed to combine the thin film technology and micromachining to fabricate a nanostructured probe or improve the surface quality and the cone angle [8–10]. The etching process in some cases has been modified to achieve a better control of the tip shape. The dynamic etching, for example, consists in moving up and down the fiber during the etching and it has proved to produce larger cone angles [11]. A more complicated method uses special optical fibers with a multistep refractive index profile and gives a more controlled shape of the tip [12]. A special and interesting etching method is the so-called *Tube Etching* (TE) [13] that improves the reproducibility, the cone angles, while reducing the roughness of the tip surface. It is quite similar to the Turner Etching but the fiber is etched without stripping the jacket. The tip grows up inside the jacket that acts as a capillary. As the etching proceeds in the up direction, the tip surface is preserved from external perturbations and becomes smoother, hence assuring the good performances of the method.

Here, we report on a TE improvement that consists in inserting vertically the fiber in the etching solution from the bottom of the growing cell (reverse tube etching, RTE). This single step method not only preserves the simplicity, the low cost and the smoothness of the etched surface typically obtained by means of the standard TE but it also guarantees a larger tip cone angle.

2. Experiment

To check the method we use multimode optical fibers (3M, FT-200-UMT), with a 200 μm core diameter, a hard polymer cladding (TECS©) of 250 μm diameter and a jacket of 500 μm diameter. The etching apparatus is made of a *Teflon* chamber equipped with two sapphire windows on the opposite sides. The windows allow the process monitoring and a precise positioning of the fiber inside the solution. Images from the inside of the chamber are collected by a CCD and stored on a PC. The bottom of the chamber is equipped with a Teflon cylinder that runs up and down driven by a micro-motor. The cylinder contains the fiber holder and the system is sealed by whole Teflon o-rings to avoid acid loss. Another fiber holder is plugged at the top of the chamber to allow the TE while the fiber is protected by the acid attack with a thick floating polymer layer (isooctane). For the RTE, a chloroform layer provides the protecting layer on the bottom of the solution, its specific weight being higher compared to the acid.

We have first investigated the HF permeability properties of the cladding and the jacket. The experiment has been carried out by dipping the fiber upside down into a chloroform–HF (30%) solution, for several hours, leaving the free apex of fiber in air outside the solution. The cladding permeability has been checked by dipping the fiber after stripping the jacket, while for the jacket permeability investigation, we dip the fiber as is. With an optical microscope we have observed that the fiber without the jacket has been etched while the fiber with the jacket was integral. This points out that the cladding has a good permeability while the jacket is acid proof. Thus, to avoid the lateral acid diffusion during the etching [13], we use the fiber with its jacket. The etching process is always completed in about 100 min at room temperature. The probes obtained were stripped, washed in an ultrasonic bath with deionized water, and finally observed by an optical microscope to evaluate the cone angles and the roughness of tip surface.

3. Results and discussion

To test the process quality, we have produced two groups of 10 fibers each, in the normal mode and in the reversed mode, respectively, comparing the average angles obtained. This double work is required because both the

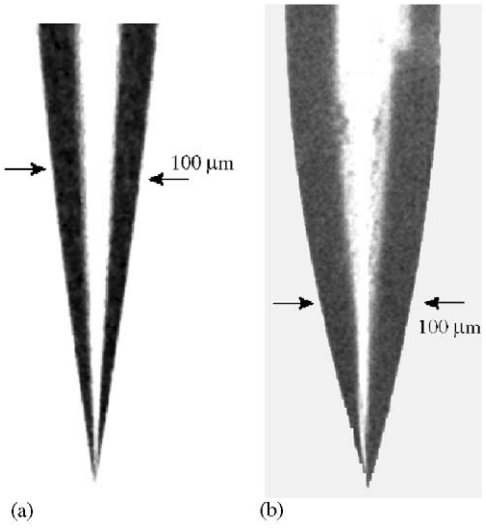

Fig. 1. Optical images of SNOM probes produced by TE (a) and by RTE (b) in the same experimental conditions.

cone angle and the roughness of the surface depend on the acid concentration, on the process temperature and on the fiber material [13]. Two groups of fibers treated in the same experimental conditions, give a precise idea of the process efficiency. Fig. 1a shows the optical image of a typical tip obtained in the normal TE. It has a regular surface and a cone angle of about 15°. The same surface quality is obtained in the RTE, as shown in Fig. 1b. Here, the cone angle is remarkably wider of about 25°.

The TE process has been described by Stökle et al. [13] with a model based on a combination of convection and diffusion occurring inside the jacket. By starting from their considerations and from our experimental results, we propose here a simple model which takes into account the gravity to explain the increase of the cone angle in the RTE. The presence of a stationary gravitational field in a liquid mixture induces a concentration gradient leading to a mass flux named barodiffusion [14]. In the TE process the acid convective flux that attacks the core surface is resolved into a radial component J_{Nrconv} and a vertical component J_{Nzconv}. Such vectorial decomposition is justified as long as the chemical etching remains a linear process. Since we have observed that the final effect of the etching is approximately linear, as proved by the probe surface shape of Fig. 1a and b, the causes must be linear too, according to the *Curie principle*.

According to Ref. [13], at the core–acid interface the following chemical reactions take place:

$$\mathrm{SiO_2} + 4\mathrm{HF} \rightarrow \mathrm{SiF_4} + 2\mathrm{H_2O},$$

$$3\mathrm{SiF_4} + 2\mathrm{H_2O} \rightarrow \mathrm{SiO_2} + \mathrm{H_2SiF_6}. \quad (1)$$

Hence, as shown in Fig. 2a a spatial gradient and an exit flux are generated. The fluxes generated inside the capillary tube are mainly due to a diffusive and a convective component [13] and, to take in account the effects of the gravity, a component $\widetilde{J}_{\mathrm{bardiff}}$ due to a barodiffusion has to be added.

The *barodiffusion* component has the following expression [14]:

$$\widetilde{J}_{\mathrm{bardiff}} = \rho D \frac{k_{\mathrm{p}}}{p_{\mathrm{I}}} \nabla p, \quad (2)$$

where ρ is the mass density of the product, D is the mutual diffusion coefficient, k_{p} is the barodiffusion ratio, p_{I} is the hydrostatic pressure inside the capillary (mainly due to the hydrofluoric acid) and ∇p is the pressure gradient containing the gravity force.

By considering as positive the direction of entering fluxes, from the chemical physical point of view we can define an *effective* convection flux along z, $J_{\mathrm{Nzconv(Ef)}}$, and along r, $J_{\mathrm{Nrconv(Ef)}}$. These represent the amount of acid that effectively etches the fiber core per second. The role of the diffusive components along $z\,(\widetilde{J}_{\mathrm{zdiff}})$, $r\,(\widetilde{J}_{\mathrm{rdiff}})$, and the barodiffusive component along $z\,(\widetilde{J}_{\mathrm{bardiff}})$, is to remove the reaction products on the attacked core surface. The main effect of the diffusive components is to allow the incoming of fresh acid on the core surface not yet etched. Thus, the acid fluxes that effectively etch the core have a reversed sign with respect to the diffusive and barodiffusive fluxes that generated them. Moreover, due to the dependence of the fluxes from the diffusion coefficient, it is to be expected that their relative magnitude is almost the same, but from the experimental results we can conclude that the barodiffusion component is slightly smaller than the other diffusion components of the fluxes. The following equations hold:

$$J_{\mathrm{Nzconv(Ef)}} = J_{\mathrm{Nzconv}} + J_{\mathrm{zdiff}} + J_{\mathrm{bardiff}},$$
$$J_{\mathrm{Nrconv(Ef)}} = J_{\mathrm{Nrconv}} + J_{\mathrm{rdiff}}. \quad (3)$$

J_{Nzconv} and J_{Nrconv} are the convective acid fluxes along the z and the radial direction; J_{zdiff} and J_{rdiff}, are the acid fluxes

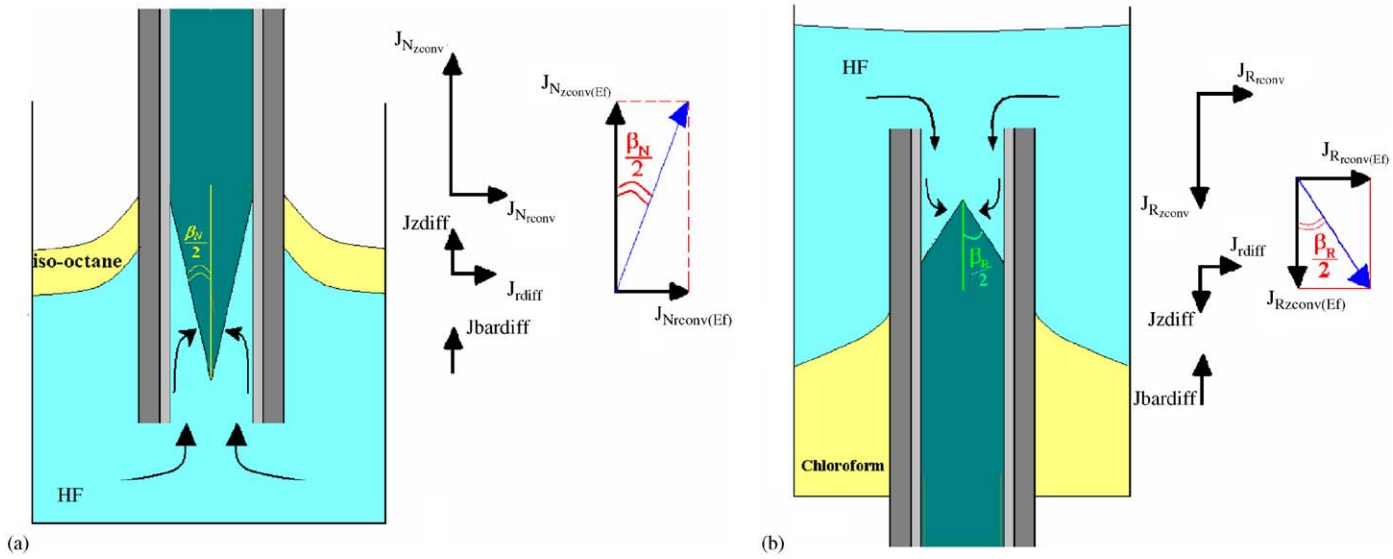

Fig. 2. Schematic diagram of the experiment for TE (a) and for RTE (b). The vectorial diagrams describe the fluxes in the two experimental geometries.

along z and the radial direction due to the diffusive processes of the reaction products.

Due to the cladding-core discontinuity and to a better *wettability* of the cladding surface, the acid etching is more favorable along the fiber walls than to center ($J_{\mathrm{Nzconv}} > J_{\mathrm{Nrconv}}$), i.e. the etching starts from the fibers walls and proceeds toward the center. In terms of etching rates (i.e. quantity of core etched per second), it means that the rate along z, $a_{\mathrm{Nz}} = \mathrm{d}z/\mathrm{d}t$, and the rate along r, $a_{\mathrm{Nr}} = \mathrm{d}r/\mathrm{d}t$, are not the same, being $a_{\mathrm{Nz}} > a_{\mathrm{Nr}}$. The tip will be completed at the time t_s, when the etching along r reaches the center of the fiber: $t_s = d/2a_r$. Within this time interval the etching along z reaches the quote $z_s = a_z t_s$, producing a conical shape of the fiber edge. The cone angle β_N depends on the etching rates along r and z as follows:

$$tg\frac{\beta_N}{2} = \frac{r_s}{z_s} = \frac{a_{\mathrm{Nr}}}{a_{\mathrm{Nz}}}. \tag{4}$$

Our simple model is able to explain why the TE is a self-limiting process [13], i.e. the pencil shape of the fiber obtained at the time t_s is not affected by the acid etching occurring for a time longer than t_s. The equation for the half shape of the probe at time t_s into the plane r–z

$$z(r, t_s) = z_s - \frac{1}{tg(\beta_N/2)} r. \tag{5}$$

Eq. (5) holds for every time $t > t_s$ (Fig. 3), since every point of the core profile is etched of the quantity a_z along z and a_r along r, the cone height z is kept constant at the value z_s. The height increase along the core sides ($a_z \cdot t$) is compensated by the height reduction in the center of the core ($-a_r/tg(\beta_N/2) \cdot t$). The geometry of the cone shape is unaffected, the only effect of the etching for $t > t_s$ being the translation of the cone in the up direction (Fig. 3).

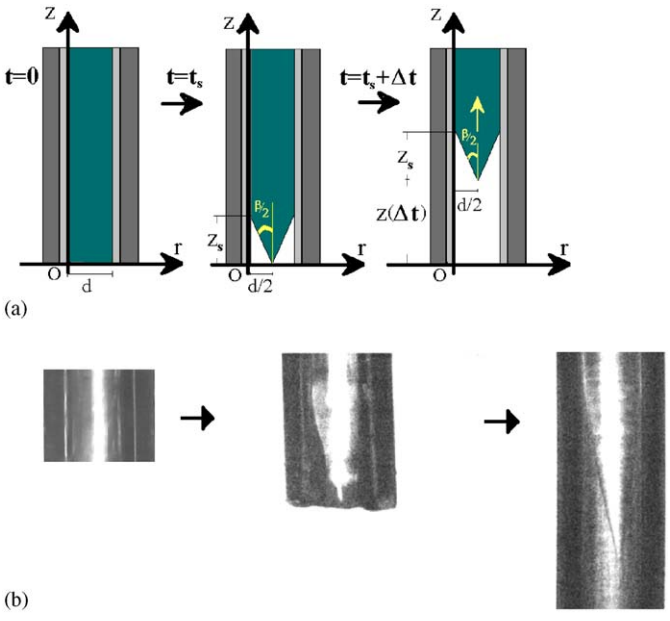

Fig. 3. Time evolution of the fiber shape as given by the model (a) and by the experiment (b).

The RTE can also be modelled by Eq. (3), provided the sign of the barodiffusion component is reversed: in this frame, the direction of the gravity force is opposite to the diffusive flux and to the convective flux directions. Hence, choosing again as positive the entering tube direction, the *effective convection* fluxes along the z and r directions become:

$$\begin{aligned} J_{\mathrm{Rzconv(Ef)}} &= J_{\mathrm{Rzconv}} + J_{\mathrm{zdiff}} - J_{\mathrm{bardiff}}, \\ J_{\mathrm{Rrconv(Ef)}} &= J_{\mathrm{Rrconv}} + J_{\mathrm{rdiff}}. \end{aligned} \tag{6}$$

J_{Rzconv} and J_{Rrconv} are the convective acid fluxes along the z and the radial direction r in the reverse frame; J_{zdiff} and J_{rdiff} are the fictitious acid fluxes along z and the radial direction due to the diffusive process of the reaction products. Eqs. (3), (4), (6) clarify the working principle of the method we have used. The barodiffusion in the reversed geometry decreases the convective flux component along the z-axis and increases the tip angle. For lower z component of the flux, the etching rate decreases in the same direction as

$$tg\frac{\beta_R}{2} = \frac{a_{\mathrm{Rr}}}{a_{\mathrm{Rz}}} > \frac{a_{\mathrm{Nr}}}{a_{\mathrm{Nz}}} = tg\frac{\beta_N}{2} \tag{7}$$

and the cone angle obtainable by RTE is higher than that obtainable by TE ($\beta_R > \beta_N$) (Fig. 2).

4. Conclusions

We reported a simple tube etching modification, named reverse tube etching, to produce SNOM probes. The method guarantees a wider angle of the probe, compared to the normal etching results. This improvement is explained by the same model describing the TE process and it is ascribed to the weakening of the effective z component of the etching flux induced by the barodiffusion. The method is easy, reliable and it represents a sensitive improvement in the low-cost production of single step etching of high throughput near-field probes.

References

[1] B. Hecht, B. Sick, U.P. Wild, V. Deckert, R. Zenobi, O.J.F. Martin, D.W. Pohl, J. Chem. Phys. 112 (18) (2000) 7761.
[2] G.K. Valaskovic, M. Holton, G.H. Morrison, Appl. Opt. 34 (7) (1995) 1215.
[3] D.R. Turner, Etch procedure for optical fibers, US patent 4,469,554 (5/4/1983);
A. Sayah, C. Philipona, P. Lambelet, M. Pfeffer, F. Marquis-Weible, Ultramicrography 71 (1998) 59.
[4] T. Held, S. Emonin, O. Marti, O. Hollricher, Rev. Sci. Instrum. 71 (2000) 3118.
[5] L. Novotny, D. Pohl, B. Hecht, Opt. Lett. 20 (1995) 970.
[6] D. Zeisel, S. Nettesheim, B. Dutoit, R. Zenobi, Appl. Phys. Lett. 68 (1996) 2491.
[7] J.F. Wolf, P.E. Hillner, R. Bilewicz, P. Kolsch, J.P. Rabe, Rev. Sci. Instrum. 70 (1999) 2751.

[8] D. Drews, W. Ehrfeld, M. Lacher, K. Mayr, W. Noell, S. Schmitt, M. Abraham, Nanotechnology 10 (1999) 61.
[9] W. Noell, M. Abraham, K. Mayr, A. Ruf, J. Barenz, O. Hollricher, O. Marti, P. Gunther, Appl. Phys. Lett. 70 (1997) 1236.
[10] T. Yatsui, M. Kourogi, M. Ohtsu, Appl. Phys. Lett. 73 (15) (1998) 2090.
[11] A. Lazarev, N. Fang, Q. Luo, X. Zhang, Rev. Sci. Instrum. 74 (8) (2003) 3679.
[12] S. Mononobe, T. Saiki, T. Suzuki, S. Koshihara, M. Ohtsu, Opt. Commun. 146 (1998) 45.
[13] R. Stöckle, C. Fokas, V. Deckert, R. Zenobi, B. Sick, B. Hecht, U.P. Wild, Appl. Phys. Lett. 75 (2) (1999) 160.
[14] L.D. Landau, E.M. Lifshitz, Fluid Mechanics, second ed., Pergamon, Oxford, 1987.